Aquaporin-0 Targets Interlocking Domains to Control the Integrity and Transparency of the Eye Lens

Woo-Kuen Lo,[1] Sondip K. Biswas,[1] Lawrence Brako,[1] Alan Shiels,[2] Sumin Gu,[3] and Jean X. Jiang[3]

[1]Department of Neurobiology, Morehouse School of Medicine, Atlanta, Georgia
[2]Department of Ophthalmology and Visual Sciences, Washington University School of Medicine, St. Louis, Missouri
[3]Department of Biochemistry, University of Texas Health Science Center, San Antonio, Texas

Correspondence: Woo-Kuen Lo, Department of Neurobiology, Morehouse School of Medicine, 720 Westview Drive SW, Atlanta, GA 30310; wlo@msm.edu.

Submitted: October 4, 2013
Accepted: January 8, 2014

Citation: Lo W-K, Biswas SK, Brako L, Shiels A, Gu S, Jiang JX. Aquaporin-0 targets interlocking domains to control the integrity and transparency of the eye lens. *Invest Ophthalmol Vis Sci*. 2014;55:1202–1212. DOI: 10.1167/iovs.13-13379

Purpose. Lens fiber cell membranes contain aquaporin-0 (AQP0), which constitutes approximately 50% of the total fiber cell membrane proteins and has a dual function as a water channel protein and an adhesion molecule. Fiber cell membranes also develop an elaborate interlocking system that is required for maintaining structural order, stability, and lens transparency. Herein, we used an AQP0-deficient mouse model to investigate an unconventional adhesion role of AQP0 in maintaining a normal structure of lens interlocking protrusions.

Methods. The loss of AQP0 in AQP0$^{-/-}$ lens fibers was verified by Western blot and immunofluorescence analyses. Changes in membrane surface structures of wild-type and AQP0$^{-/-}$ lenses at age 3 to 12 weeks were examined with scanning electron microscopy. Preferential distribution of AQP0 in wild-type fiber cell membranes was analyzed with immunofluorescence and immunogold labeling using freeze-fracturing transmission electron microscopy.

Results. Interlocking protrusions in young differentiating fiber cells developed normally but showed minor abnormalities at approximately 50 μm deep in the absence of AQP0 in all ages studied. Strikingly, protrusions in maturing fiber cells specifically underwent uncontrolled elongation, deformation, and fragmentation, while cells still retained their overall shape. Later in the process, these changes eventually resulted in fiber cell separation, breakdown, and cataract formation in the lens core. Immunolabeling at the light microscopy and transmission electron microscopy levels demonstrated that AQP0 was particularly enriched in interlocking protrusions in wild-type lenses.

Conclusions. This study suggests that AQP0 exerts its primary adhesion or suppression role specifically to maintain the normal structure of interlocking protrusions that is critical to the integrity and transparency of the lens.

Keywords: aquaporin-0, lens, interlocking domain, AQP0-deficient mice, adhesion

The lens is composed of numerous sheets of slender fiber cells covered by a monolayer of epithelium at its anterior surface. The transparent lens permits incident light to pass through and help form a focused image on the retina through the mechanism of visual accommodation. The lens possesses several unique features to serve these specific functions. During postnatal lens development, the epithelial cells at the equatorial region continuously divide and differentiate into new fiber cells, and all fiber cells of different ages are retained within the lens throughout the entire life span. All lens cells contain a high concentration of crystallin proteins for increasing the refractive index. The mature fiber cells in the deeper region lose their organelles during the maturation process to eliminate light scattering. Furthermore, fiber cell membranes undergo a number of specializations to accommodate these special needs. One of the major membrane specializations is that fiber cell membranes develop an elaborate interlocking system[1–3] that is required for maintaining the structural order, stability, and lens transparency, especially during the deformation associated with visual accommodation.

The interlocking system between fiber cells is basically in the forms of protrusions and balls and sockets in various species studied.[1–5] The protrusions are located at the corners (angles) of hexagonal fiber cells, whereas the balls and sockets are distributed on the narrow and broad sides of fiber cells.[1–3,5,6] The interlocking protrusions are distributed extensively in the cortical and nuclear fibers of the lens.[1–3,6–8] They normally consist of the narrowed neck and expanded head portions, with the head diameter in the range of 0.5 to 2 μm. Other terms such as *interdigitations*, *spikes*, and *interlocking devices* have also been used to describe the same structure.[1,2,6,9,10] The interlocking protrusions have a major role in maintaining fiber cell stability that is crucial for lens transparency and visual accommodation. Because balls and sockets are associated with gap junctions, they are believed to have a role in facilitating microcirculation of ions and small substances between fiber cells.[5]

The major intrinsic protein (MIP), which consists of approximately 50% of the total integral fiber cell membrane proteins in the lens, has been extensively studied in the past 40 years.[11–17] MIP was initially suspected to be a gap junction

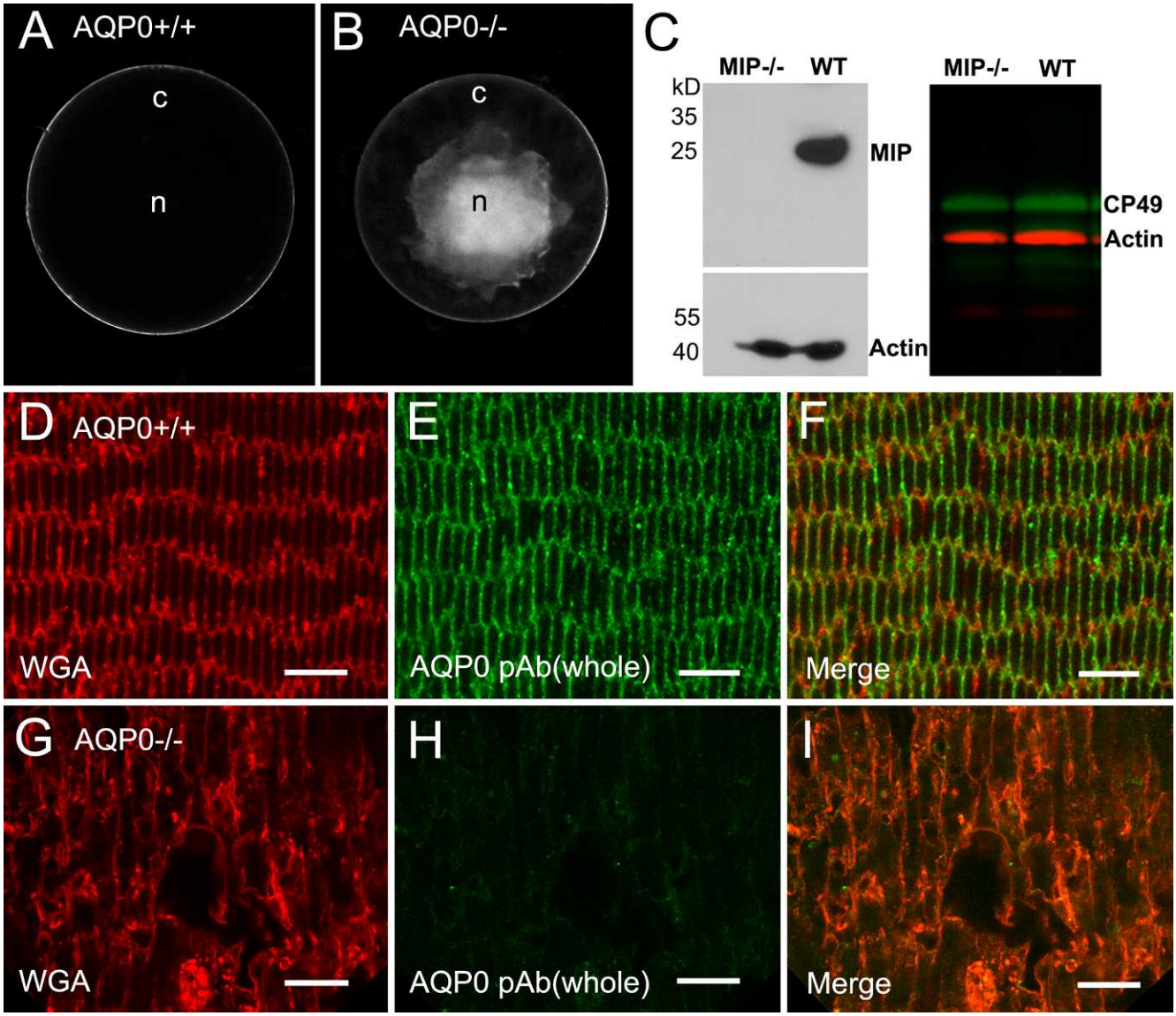

Figure 1. Formation of nuclear cataract and loss of AQP0 protein in an AQP0-deficient lens. (**A**, **B**) The wild-type control displays a whole transparent lens compared with the appearance of dense cataract in the lens core in the AQP0$^{-/-}$ lens at age 5 weeks. (**C**) The absence of AQP0 proteins in AQP0$^{-/-}$ fiber cell membrane preparations is determined by Western blot (*left*). The presence of the CP49 beaded filament proteins is detected in both AQP0$^{-/-}$ and wild-type lenses with Western blot (*right*). By confocal immunofluorescence, labeling of AQP0 polyclonal antibody is present in cortical fiber cell membranes in the wild-type control (**D–F**), but is absent in the AQP0$^{-/-}$ cortical fibers (**G–I**). Note that swollen fiber cells are shown in the AQP0$^{-/-}$ lens. Rhodamine-conjugated wheat germ agglutinin was used to delineate the fiber cell membrane outlines. *Scale bars*: 5 μm.

protein[18–20] and was later identified as a water channel protein, aquaporin-0 (AQP0), in 1995 by Mulders and associates.[21] A number of mutations in AQP0 are directly associated with various forms of cataracts in humans and animals.[22–28]

Although studies have shown that AQP0 proteins possess several unique channel properties different from those of other members of the aquaporin family,[21,29–33] including AQP1 in the epithelial cells of the same lens,[29] its water channel function in the lens fibers has been established in several species studied.[29,30,32,34–36] However, it has been shown that the channels of AQP0 proteins are closed upon cleavage of their C-terminals to form junctions.[33,37–41] The AQP0-dependent thin junctions and wavy square array junctions are also formed regularly in different regions of the intact lens.[42–46] In addition, in vitro studies[47,48] have shown the increased cell-cell adhesion in cells overexpressing AQP0. Subsequently, the new, unconventional adhesion role of AQP0 in the lens has become a novel subject of investigation.[37,39,45–50]

In this study, we report that interlocking protrusions are particularly enriched with AQP0. In contrast to the wild-type lens with a well-defined structure, the interlocking protrusions of cortical fibers in the AQP0-deficient lens specifically undergo uncontrolled elongation, deformation, and fragmentation, which lead to fiber cell separation, breakdown, and cataract formation in the lens core. Herein, we uncovered a novel function of AQP0 specifically in maintaining a normal structure of interlocking protrusions that is critical to the integrity and transparency of lens fiber cells.

Investigative Ophthalmology & Visual Science

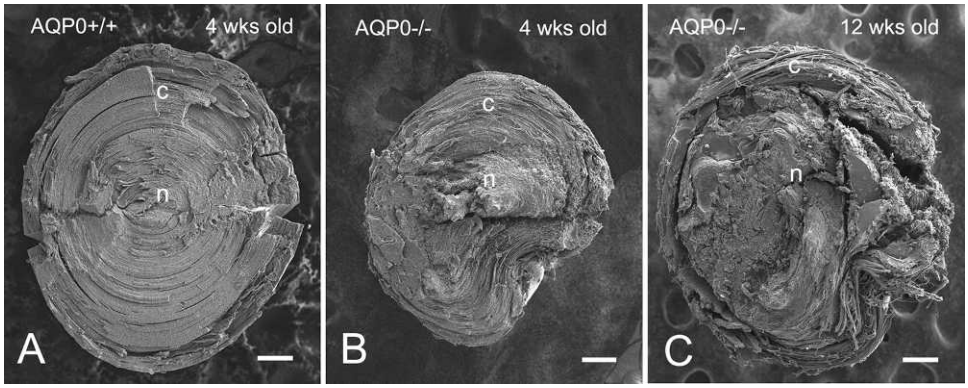

Figure 2. Fractured fiber cell surfaces differ between wild-type and AQP0$^{-/-}$ lenses. (**A**) By SEM, midsagittal fractured surfaces show the presence of intact fibers in both cortex (c) and nucleus (n) in the wild-type lens at age 4 weeks. (**B**, **C**) In contrast, only remnant layers of intact fibers in the superficial cortex and damaged fibers in the lens nucleus are seen in the AQP0$^{-/-}$ lenses at age 4 weeks and age 12 weeks. The size of the AQP0$^{-/-}$ lens at age 4 weeks is approximately 10% smaller than that of the wild type, while the AQP0$^{-/-}$ lens at age 12 weeks is comparable to the 4-week-old wild type (see the Results section). *Scale bars*: 200 μm.

Methods

Animals and Lens Transparency Photography

The *MIP*/AQP0-deficient mice[51] and the wild-type mice were bred and maintained in accordance with a protocol approved by the Institutional Animal Care and Use Committee at the University of Texas Health Science Center, San Antonio, Texas. The *Mip*-null mice are originally maintained on a mixed 129/C57B6-J background and are therefore not null for CP49. While breeding the original mice, the pairs that were wild type (C57B6-J) at the CP49 locus were selected to rescue the CP49 deletion carried by the 129 strain. The deep sequencing (RNA sequence) data show that the transcript levels for CP49/BFSP2 in *Mip*$^{-/-}$ lenses (P7) are approximately 96% of wild type (C57B6-J).[51] The presence of CP49 beaded filament proteins in the AQP0$^{-/-}$ lenses was further confirmed in this study by Western blot (see below). All studies were conducted in strict accordance with the Association for Research in Vision and Ophthalmology Resolution on the Use of Animals in Research. Freshly isolated lenses of AQP0$^{-/-}$ and wild-type mice at age 3 to 12 weeks were collected in M-199 or PBS solution at room temperature (RT) for documenting their transparency under a dissecting microscope (Nikon SMZ800, Tokyo, Japan) equipped with a digital camera (Nikon Coolpix 5000, Tokyo, Japan). Lenses were then prepared for Western blot analysis or fixed in the fixative for the various experiments described below.

Western Blot Analysis

Lens membrane protein preparation was performed as previously described.[52] Briefly, tissue lysates were prepared by homogenizing lenses of AQP0$^{-/-}$ and wild-type mice in lysis buffer (5 mM Tris, 5 mM EDTA, 5 mM EGTA, 250 mM sucrose, and protease inhibitors). The lens lysates were centrifuged at 100,000*g* at 4°C for 30 minutes. The pellets were resuspended in 20 mM sodium hydroxide and centrifuged again at 100,000*g* at 4°C for 30 minutes. The pellets were resuspended, and protein concentrations were determined using the Micro BCA Protein Reagent assay kit (Pierce, Rockford, IL). Thirty micrograms of protein was loaded, separated on a 10% SDS-PAGE, and transferred to a nitrocellulose membrane. The membranes were immunoblotted with affinity-purified antibodies for mouse AQP0 (1:300 dilution) and β-actin (1:5000 dilution). Secondary antibodies conjugated with horseradish peroxidase, anti-rabbit antibody (1:5000 dilution) for mouse AQP0, and anti-mouse antibody (1:5000 dilution) for β-actin were used to detect primary antibodies. The signals were detected using an Amersham ECL chemiluminescence reagent kit (GE Healthcare Bio-Sciences, Pittsburgh, PA) and X-OMAT AR films (Eastman Kodak, Rochester, NY).

For detecting CP49 beaded filament proteins, lenses from both AQP0$^{-/-}$ and wild-type mice were dissected, and the cortical parts were isolated. The water-insoluble fractions containing the membrane and cytoskeletal proteins were prepared using a modified procedure.[53] Thirty-microgram proteins were loaded, separated by SDS-PAGE, and probed with Western blot as described above. An affinity-purified rabbit anti-CP49 antibody (1:1000 dilution; C1 anti-CP49, a gift from Paul FitzGerald of the University of California, Davis, CA) and mouse anti–β-actin antibody (1:5000 dilution) were used as primary antibodies. IRDye 800CW goat anti-rabbit IgG (labeled green) and IRDye 680RD goat anti-mouse IgG (labeled red; LI-COR Biosciences, Lincoln, NE) were used as secondary antibodies.

Confocal Immunofluorescence Labeling

Eye lenses were freshly removed from wild-type mice after euthanasia and were fixed immediately in 4% paraformaldehyde (EMS, Hatfield, PA) in PBS for 2 hours at RT. We used whole-mount preparations to conduct confocal immunofluorescence labeling to obtain longitudinal views of the elongated cortical fiber cells. To prepare whole-mount cortical fiber cells, we first cut the lens into quarters with a double-edged razor blade along the anterior to posterior axis. In each quarter, the entire lens nuclear region was removed with tweezers, and the remaining successive layers of cortical fibers were gradually peeled away until the desired approximate layers of cells were achieved as determined by degrees of transparency under a dissecting microscope with a light source from the bottom.

For labeling of AQP0 antibody, quarters of fiber cells in slightly different layers were incubated in 2% BSA-PBS solution for 1 hour at RT to block nonspecific binding. They were then incubated with the affinity-purified rabbit anti-bovine AQP0 polyclonal antibody[20] (a gift from Ross Johnson of the University of Minnesota, Minneapolis, MN) or the rabbit anti-human AQP0 C-terminal affinity-purified polyclonal antibody (Alpha Diagnostic, San Antonio, TX) at 1:300 dilution in the blocking solution for 2 hours at RT or overnight at 4°C. After washing (twice for 10 minutes each) in PBS, fiber cell whole mounts were incubated with FITC-conjugated or rhodamine-conjugated goat anti-rabbit IgG secondary antibody at 1:200

Investigative Ophthalmology & Visual Science

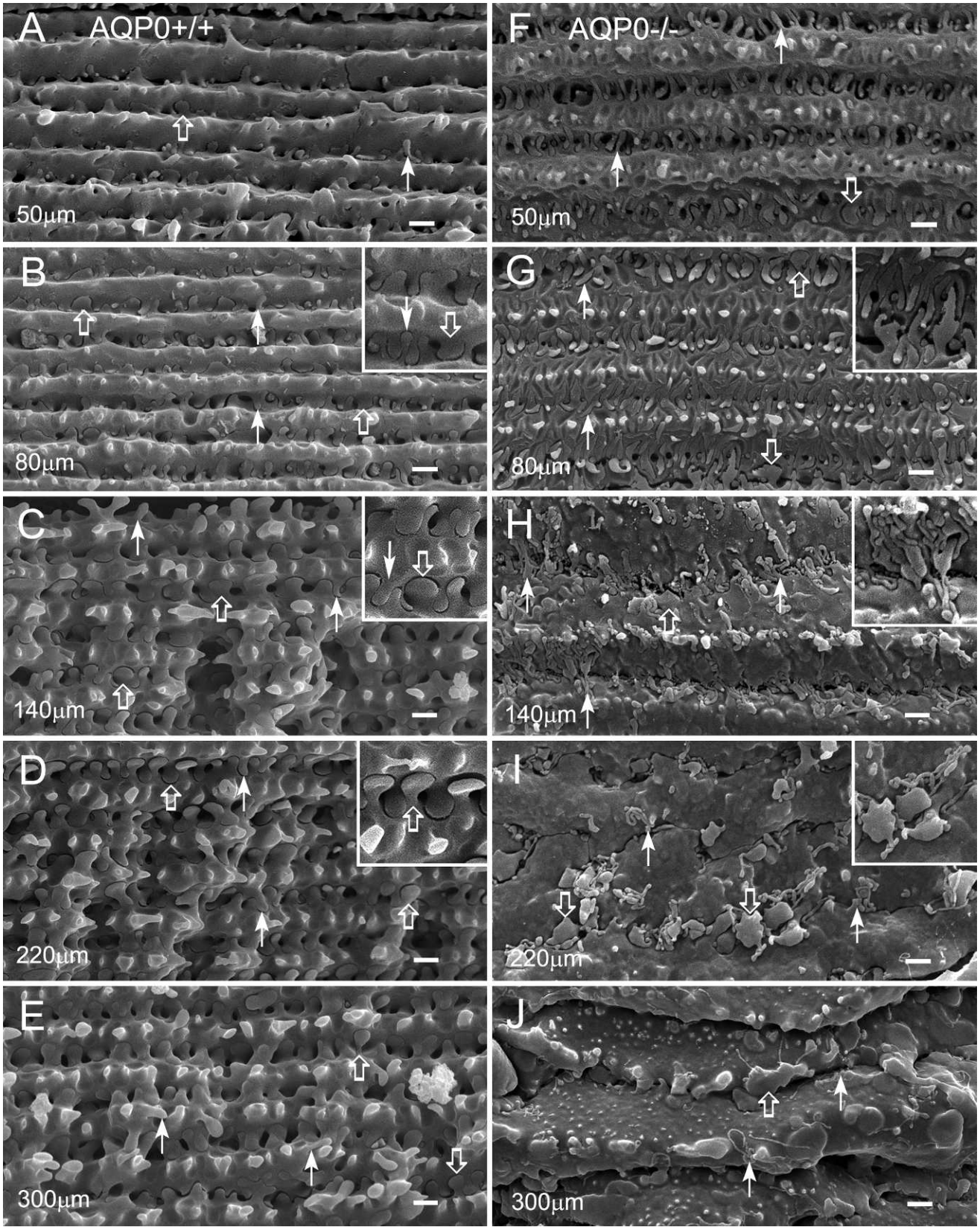

Figure 3. Interlocking protrusions exhibit dramatic structural changes as fiber cells mature in an AQP0$^{-/-}$ lens. Structural comparisons of protrusions are made from the narrow-side fiber cells in different cortical regions between the wild type and AQP0$^{-/-}$ at age 4 weeks. (**A–E**) In wild-type lenses, interlocking protrusions (50–300 μm deep from the equatorial surface) undergo various stages of development and maturation. Many small protrusions are seen at approximately 50 μm in the superficial cortex (**A**). They grow and mature into unique configurations in deeper mature cortical fibers (**B–E**). Typically, two different configurations of protrusions are identified based on their unique shapes (see the insets in [**B–D**]). Type 1 normally consists of a narrowed neck and expanded head portions, with the head diameter in the range of 0.5 to 2 μm (*open arrows*). Type 2

Investigative Ophthalmology & Visual Science

generally displays a slender, tubular shape, with a diameter of approximately 0.1 to 0.3 μm (*arrows*). (**F–J**) In an AQP0$^{-/-}$ lens, protrusions of both types undergo similar stages of formation and growth but show signs of minor abnormalities at approximately 50 μm deep in the absence of AQP0 (**F**). As fiber cells mature, these protrusions surprisingly undergo uncontrolled elongation ([**G**, **H**] and insets), deformation (insets in [**H**, **I**]), and breakdown (**I**, **J**). Severe deformation of the protrusions eventually results in separation and collapse of fiber cells (**I**, **J**). *Scale bars*: 1 μm.

dilution (Jackson ImmunoResearch Laboratories, West Grove, PA) for 1 hour at RT, rinsed in PBS, and examined with a Zeiss LSM 700 confocal microscope (Carl Zeiss, Oberkochen, Germany).

Scanning Electron Microscopy

Freshly isolated lenses of AQP0$^{-/-}$ and AQP0$^{+/+}$ mice were fixed in 2.5% glutaraldehyde in 0.1 M cacodylate buffer (pH 7.3) at RT for 48 to 72 hours. Each lens was properly oriented and fractured with a needle to expose the narrow or broad side of the membrane surfaces of hexagonal fiber cells. Lens halves were postfixed in 1% aqueous osmium tetroxide for 1 hour at RT, dehydrated in graded ethanol, and dried in a critical point dryer (Tousimis, Rockville, MD). Lens halves were oriented and mounted on specimen stubs and coated with gold/palladium in a sputter coater (Anatech, Union City, CA). Micrographs were taken with a JEOL 820 scanning electron microscope (JEOL USA, Inc., Peabody, MA) at 10 kV.

Freeze-Fracturing Replica Immunogold Labeling

We followed the same procedures as described previously.[5] Briefly, freshly isolated wild-type mouse lenses were lightly fixed in 0.75% paraformaldehyde in PBS for 30 minutes at RT and cut into 300-μm slices with a vibratome (Vibratome 1000 Plus; Ted Pella, Redding, CA) to make freeze-fracturing replicas. One drop of 0.5% parloidion in amyl acetate was used to secure the integrity of a large replica during cleaning and labeling procedures. The replica was washed with 2.5% sodium dodecyl sulfate, 10 mM Tris-hydrochloride, and 30 mM sucrose (pH 8.3) at 50°C until all visible attached tissue debris was removed from the replica. The replica was then rinsed with PBS, blocked with 4% BSA–0.5% teleostean gelatin in PBS for 30 minutes, and incubated with the rabbit anti-bovine AQP0 whole serum antibody (provided by Ross Johnson of the University of Minnesota, Minneapolis, MN) at 1:10 dilution for 1 hour at RT. The replica was washed with PBS and incubated with 10 nm Protein A Gold (EY Laboratories, Inc., San Mateo, CA) at 1:50 dilution for 1 hour at RT. After rinsing, the replica was fixed in 0.5% glutaraldehyde in PBS for 10 minutes, rinsed in water, collected on a 200-mesh Gilder Finder Grid (Electron Microscopy Sciences, Hatfield, PA), rinsed with 100% amyl acetate for 30 seconds to remove parloidion, and viewed with a JEOL 1200EX transmission electron microscope (JEOL USA, Inc.).

Quantitative analysis of the AQP0 distribution in protrusions versus nonprotrusion flat cell membranes was performed on micrographs at ×40,000 taken randomly from three replicas prepared from three animals of similar age. Each protrusion and nonprotrusion area (in micrometers squared) was measured from each micrograph with the Zeiss AxioVision LE 4.7 (Carl Zeiss) on a personal computer (HP Compaq DC7900, Palo Alto, CA), and the number of gold particles was counted manually with a cell counter. The number of gold particles per 1-μm^2 surface area of these two individual domains was calculated from each micrograph. The average number of gold particles per 1-μm^2 surface area of these two individual domains was obtained from each replica. Statistical comparisons of the averages were made by Student's *t*-test using the software program SPSS 14.0 (SPSS, Inc., Chicago, IL). $P < 0.05$ was considered significant.

Results

Absence of AQP0 Disrupts Structural Organization of Lens Fibers

As previously reported[22,48] and unlike the controls (Fig. 1A), AQP0-deficient mice in all ages examined displayed dense opacity in the lens nuclear regions (Fig. 1B). The size of nuclear opacity was usually increased with age by extension toward the cortical regions. In addition, cataractous lenses were approximately 10% smaller compared with their same-age controls (Figs. 1A, 1B). The estimated size of AQP0$^{-/-}$ lenses was measured from the diameter between the lens equators on the fractured surfaces of three pairs of lenses at age 1 month. The absence of AQP0 proteins in the lenses from the AQP0-deficient mouse colony used in this study was further confirmed by Western blot (Fig. 1C) and immunofluorescence labeling (Figs. 1D–I) using a specific AQP0 polyclonal antibody. The fiber cells in the outer cortex were significantly swollen and disorganized in the AQP0-deficient lens (Fig. 1G) compared with the control (Fig. 1D).

Because *Mip*$^{-/-}$ mice are originally maintained on a mixed 129/C57B6 background, we have therefore taken an additional step to make sure that the AQP0$^{-/-}$ lenses used in this study contained CP49 beaded filament proteins.[54,55] The presence of comparable levels of CP49 proteins was indeed confirmed in the AQP0$^{-/-}$ and wild-type lenses with Western blot analysis (Fig. 1C), and immunofluorescence labeling (data not shown).

The morphologic changes in fiber cell surface associated with the loss of AQP0 were examined in detail with scanning electron microscopy (SEM). When the fractured surface of the lens was viewed from the equatorial surface toward the lens core, consecutive layers of elongating fiber cells contained sequential ages of differentiated fiber cells, with the younger cells located superficially and the older ones deeper. This unique age-related cell layer arrangement enabled us to make precise examinations of the chronicled changes in surface morphology during fiber cell differentiation and maturation in both AQP0-deficient and wild-type control mice. The lenses from the control and AQP0$^{-/-}$ mice were examined under low magnification (Fig. 2). In the 4-week-old control, intact fibers were regularly observed in both cortical and nuclear regions (Fig. 2A). In contrast, similar intact fibers were seen only in the cortical region, approximately 200 μm deep, in the AQP0$^{-/-}$ lens at the same age (Fig. 2B). At age 12 weeks, only a significantly narrower superficial cortical region (e.g., ≤100 μm) contained intact fibers (Fig. 2C). A complete breakdown of nuclear fibers was observed in all ages examined. While new fiber cells still formed in the equatorial superficial cortex, continued accumulation of damaged cortical fibers on top of disrupted nuclear fibers resulted in an increase in the size of the total damaged cell mass in the lens core seen in the 12-week-old lens (Fig. 2C).

Interlocking Protrusions Develop Normally in Young Differentiating Fiber Cells in the Absence of AQP0

The interlocking protrusions began to develop in newly differentiating fiber cells in a few layers deep in the wild-type lenses at all ages studied (Fig. 3). As fiber cells continued to

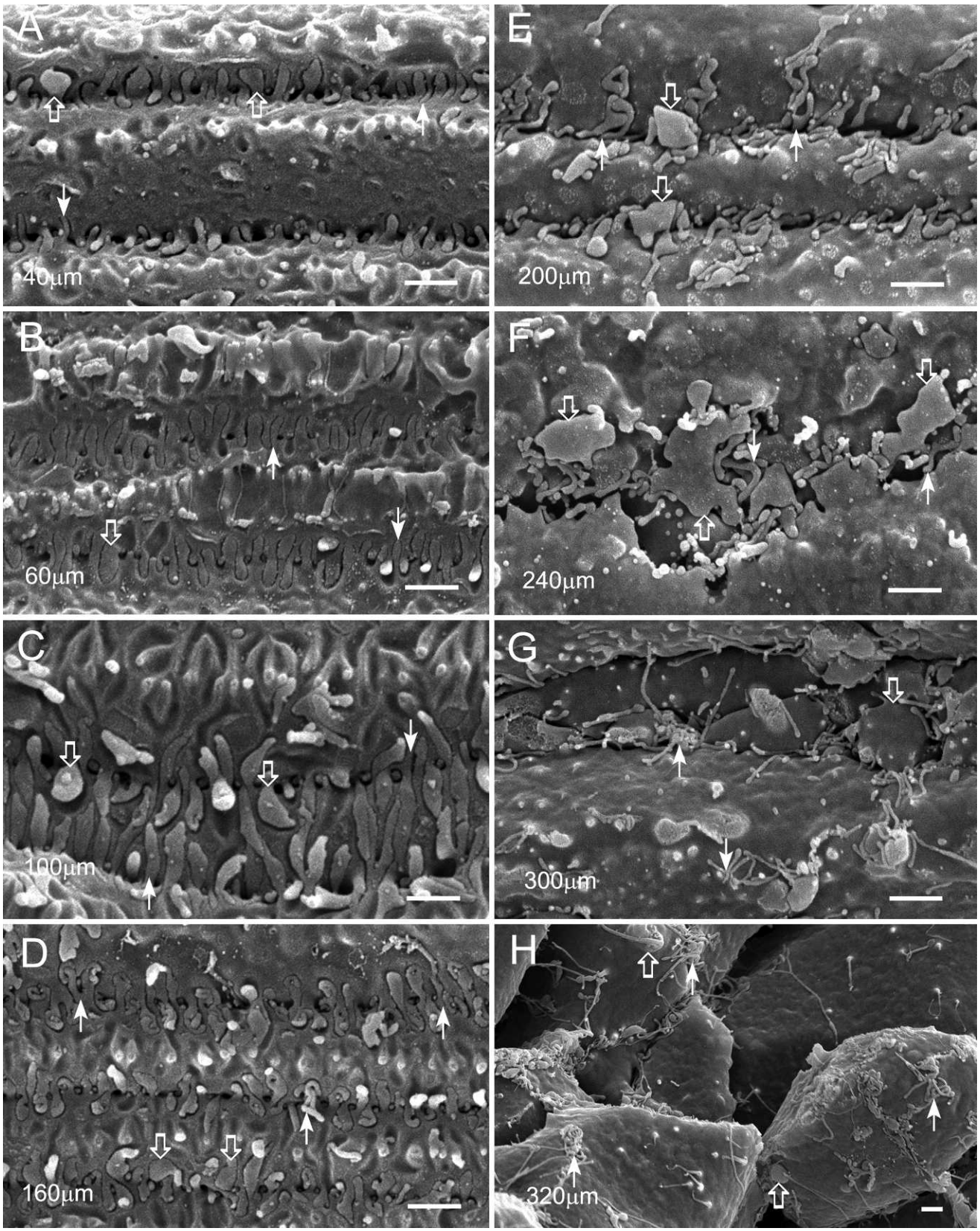

Figure 4. A detailed sequence of events for uncontrolled elongation, deformation, and breakdown of protrusions in an AQP0$^{-/-}$ lens. (**A**, **B**) The normal formation of two types of protrusions occurs in the absence of AQP0 in young differentiating fibers that may be seen at approximately 40 μm deep (**A**), but show signs of abnormal elongation at approximately 60 μm deep (**B**). Under this condition, type 1 (*open arrows*) and type 2 (*arrows*) elongated protrusions still exhibit their typical structural characteristics and interlock with each other in a tightly compact fashion (**B**). (**C**, **D**) In deeper fibers at approximately 100 μm deep, while type 1 changes its shape and size, type 2 elongates into tubular structures of uncontrolled length. (**D**, **E**) Due to restriction of the extracellular distance between narrow-side fiber cells, many elongated tubular protrusions make recurrent

Investigative Ophthalmology & Visual Science

turns and twists to form complex aggregates. (**E**, **F**) Type 1 protrusions (*open arrows*) show significant shape changes and size increases in deeper fibers at approximately 200 μm deep. Both types of protrusions become fragmented, and the interlocking support between protrusions is completely vanished. (**G**, **H**) This eventually leads to fiber cell separation and collapse in the deeper cortex at approximately 300 μm deep. *Scale bars*: 1 μm.

grow, small newly formed interlocking protrusions were regularly seen along the sides of young differentiating fiber cells (Figs. 3A, 3B). These small protrusions gradually grew and matured into larger ones as fiber cells aged (Figs. 3C–E). In the AQP0-deficient lenses, interlocking protrusions were also formed and developed into normal shape and size in young differentiating fiber cells but showed signs of minor abnormalities at approximately 50 μm deep from the equatorial surface (Figs. 3F, 4A, 4B). Nevertheless, this may be expected because an earlier study[8] had shown that clathrin, AP-2 adapter, and actin cytoskeleton are likely to be responsible for the initial formation of interlocking domains in the lens fibers.

Loss of AQP0 Results in Uncontrolled Elongation, Deformation, and Breakdown of Maturing Protrusions, Which Cause Fiber Cell Separation and Collapse

Conversely, after the development of interlocking protrusions in the AQP0-deficient mice, a majority of protrusions in superficial fiber cells specifically began to undergo uncontrolled, excessive elongation and deformation (Figs. 3G–I, 4C, 4D), despite that the cortical fiber cells retained their normal shape initially. Uncontrolled elongation of protrusions was apparently restricted by the short distance (approximately 1.5 μm wide) and narrowed space between fiber cell surfaces; these elongated protrusions later became further twisted recurrently along the sides of fiber cells to adapt to the space constraints (Figs. 3H–J, 4D–F). These severe deformations of protrusions eventually caused the separation and breakdown of fiber cells, which lead to cataract formation in the lens core (Figs. 3J, 4F–H).

AQP0 Is Enriched in Interlocking Protrusions

Because protrusions began to undergo significant changes in their shape and size in superficial cortical regions in the absence of AQP0, it led us to investigate whether AQP0 is particularly enriched in protrusions for maintaining their structural integrity in the lens. By confocal immunofluorescence labeling, AQP0 polyclonal antibody was indeed labeled preferentially on protrusions along the borders of broadside fiber cells in superficial cortical regions, where the fiber cells generally displayed straight membrane surfaces (Fig. 5B). This labeling pattern correlated well with the distribution of protrusions seen along the straight borders of broadside fiber cells as viewed on SEM (Fig. 5A). In the deeper cortical regions, protrusions were associated with undulating borders of broadside fiber cells (Fig. 5C). Immunofluorescence analysis showed that the consistent dotted pattern of AQP0 polyclonal antibody labeling was predominantly along the undulating borders of broadside fiber cells (Fig. 5D). The COOH-terminal of AQP0 is known to be cleaved in the core region of lens fibers.[11,13,56] Immunofluorescence labeling using an AQP0 C-terminal polyclonal antibody also showed the similar labeling pattern along undulating cell borders, suggesting that the AQP0 C-terminal was also present in protrusions of slightly deeper cortical fibers (Fig. 5E).

The preferential distribution of AQP0 in interlocking protrusions was further validated with immunogold labeling of AQP0 polyclonal antibody on freeze-fracturing replicas at the electron microscopic level. In this study, we have established the specificity of AQP0 antibody labeling by showing the specific distribution of gold particles predominantly on the cell membranes but not on the cytoplasm (Figs. 6A–D). The clusters of gold particles were preferentially localized along the borders of several protrusions (Fig. 6A, arrows). Additionally, the preferential distribution of gold particles was consistently found in protrusions compared with the adjacent cell membranes (Figs. 6B–D). Furthermore, an elevated concentration of gold particles was distributed along the extracellular spaces between interlocking protrusions (Fig. 6C, arrows). This suggests that the adhesion function of AQP0 is concentrated in the extracellular loops of the molecules distributed on both membrane surfaces of the protrusions. By quantitative examination conducted on the micrographs displaying both protrusions and flat cell membranes as shown in Figure 6D, our data confirmed that protrusions have significantly more AQP0 gold particles than adjacent flat nonprotrusion membranes (Fig. 6E; $P < 0.001$). The analysis included a total of 5136 gold particles, which were counted from micrographs taken randomly from three large replicas. This quantitative result indicated that the interlocking protrusions were indeed the AQP0-rich domains that are likely to serve as adhesion sites for AQP0 to maintain the structural stability of fiber cells.

Discussion

This study demonstrated that the loss of AQP0 specifically disrupts interlocking protrusions by dramatically changing their unique structural features (i.e., shape and size) during fiber cell differentiation and maturation in cortical regions of the lens. These structural changes resulted in the loss of function for interlocking protrusions to maintain the structural integrity of cortical fiber cells and eventually led to fiber cell separation, breakdown, and cataract formation in the lens core. The present study also demonstrated that AQP0 is particularly enriched in the interlocking protrusions in mouse lenses, which is consistent with observations in earlier studies.[49,57] Taken together, these results strongly suggest that AQP0, possibly functioning as an adhesion molecule, has a critical role in maintaining the normal shape and size of interlocking protrusions. Because the static normal tubular protrusions have transformed into motile elongating filopodia-like structures in the absence of AQP0, it is also postulated that AQP0 may serve as a regulatory or suppression molecule to regulate normal features of protrusions. In view of the vast distribution of interlocking protrusions extending from the superficial cortex to the nucleus of the entire lens,[1–3,6,7,9] the functional impact of AQP0 on the structural integrity and transparency of the lens is of substantial significance.

Although interlocking protrusions are an AQP0-rich domain, AQP0 is not required for the formation of protrusions as demonstrated in the AQP0-deficient lenses in this study (Figs. 3, 4). This conclusion is partially supported by earlier findings that clathrin, AP-2 adapter, and actin cytoskeleton are specifically involved in the formation of interlocking domains.[8] The possible involvement of several other actin-based cytoskeletal proteins such as Arp2/3 complex,[58,59] formins,[60,61]

Investigative Ophthalmology & Visual Science

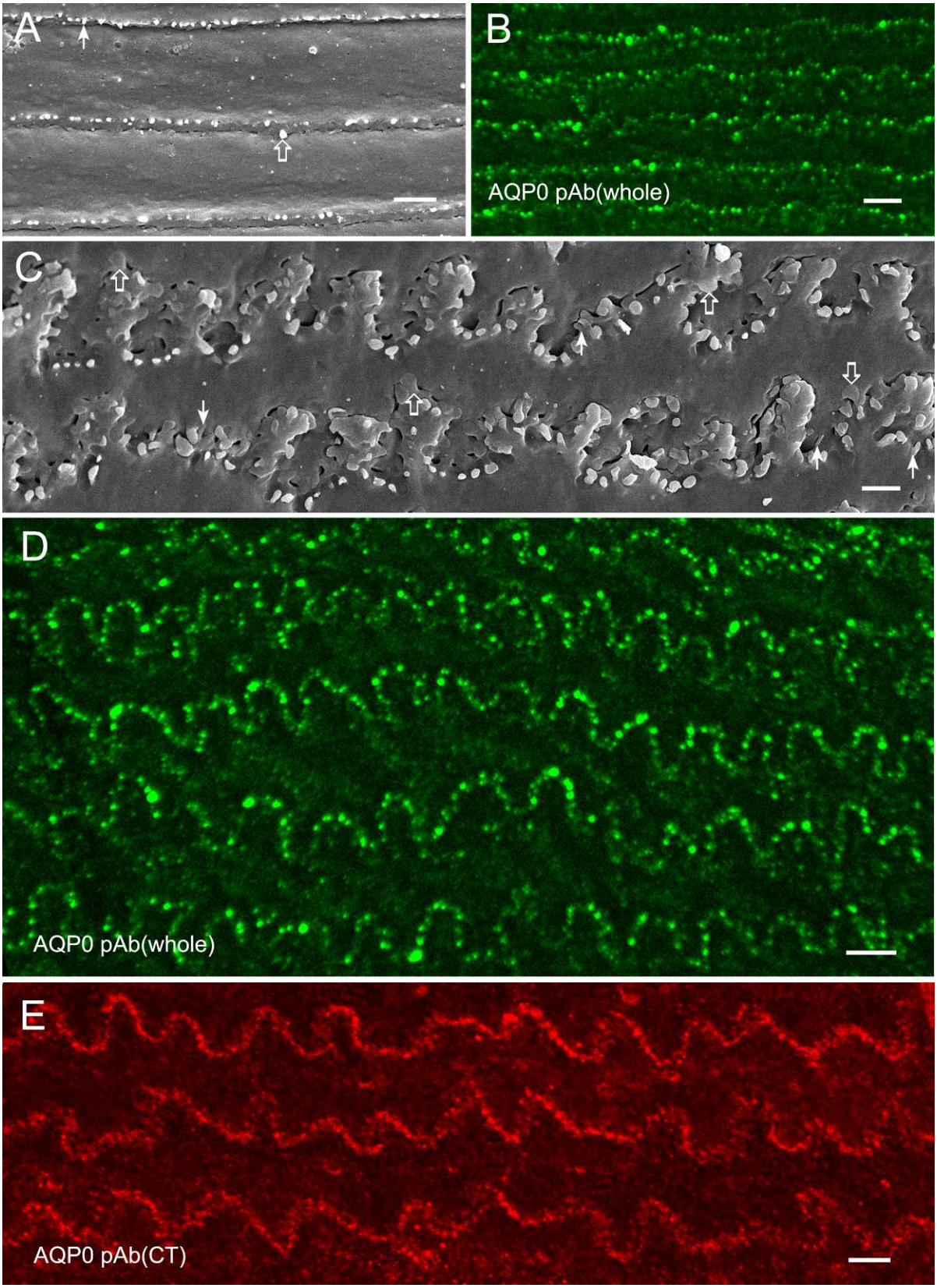

FIGURE 5. Aquaporin-0 is particularly enriched in protrusions examined with confocal immunofluorescence. (**A**) Scanning electron microscopy shows that in superficial fibers type 1 (*open arrows*) and type 2 (*arrows*) small protrusions are distributed along fairly straight broadside fiber cells in whole-mount preparations of wild-type lenses. (**B**) Immunofluorescence exhibits a dotted pattern of labeling for AQP0 polyclonal antibody against the whole molecule along the broadside superficial fiber cells, which correlates well with the straight distribution of protrusions seen on SEM. (**C**) Scanning electron microscopy shows the distribution of type 1 (*open arrows*) and type 2 (*arrows*) protrusions along the undulating boarders of broadside fiber cells in the deeper cortex. (**D**) Immunofluorescence reveals the distinct undulating dotted pattern of labeling for AQP0

Investigative Ophthalmology & Visual Science

polyclonal antibody against the whole molecule, which correlates well with the similar undulating distribution of protrusions along the broadside fiber cells in the deeper cortex seen on SEM. (**E**) Using an AQP0 C-terminal polyclonal antibody, its undulating dotted pattern of labeling is also consistent with the undulating distribution of protrusions along the broad side of deeper cortical fiber cells. *Scale bars*: 2 μm in (**A**, **C**); 5 μm in (**B**, **D**, **E**).

and ezrin[62–64] in developing and maintaining the protrusions has also been implicated. A direct interaction between AQP0 and ezrin in the lens has been reported.[64] It is possible that AQP0 acts through interactions with the underlying ERM proteins and actin cytoskeletal complex in protrusions to regulate normal features of the interlocking domains. The present study showed that in the absence of AQP0 protrusions can develop and grow normally in young differentiating fiber cells but show signs of minor abnormalities at approximately 50 μm deep from the equatorial lens surface. This suggests that the rich accumulation of AQP0 in protrusions perhaps occurs shortly after protrusions are formed through a progressive (or massive) insertion of AQP0 proteins during fiber cell differentiation. A large distribution of AQP0-containing membrane vesicles in cell cytoplasm and the transport of these vesicles along microtubules in differentiating fiber cells have been reported in an earlier study.[65]

Due to the extensive distribution of protrusions throughout the entire lens, the importance of these unique interlocking structures in maintaining the stability of fiber cells has been suggested repeatedly in earlier morphologic studies.[1–3,5,7–9] Our study for the first time to date uncovered an underlying mechanism by identifying AQP0 as a specific molecule controlling the normal structure of interlocking protrusions. This finding further manifested the fundamental importance of this structure and AQP0 to the lens.

Although our study unraveled different responses for type 1 and type 2 interlocking protrusions in the absence of AQP0 (Figs. 3, 4), it is most likely that they have similar roles in maintaining the structural stability and transparency of fiber cells. Structurally, type 1 displayed a narrowed neck with an expanded head resembling a mushroom or lamellipodia, whereas type 2 exhibited a slender, tubular shape resembling filopodia (Fig. 3). A detailed examination indicated that different combinations of interlocking patterns occurred regularly between these two protrusion types, namely, type 1 with type 1, type 2 with type 2, and type 1 with type 2 (Fig. 3). These combining interlocking patterns strongly suggested that the two protrusion types are working together cooperatively and flexibly to achieve the most effective interlocking necessary for structural stability between neighboring fiber cells based on their spatial constraints (Fig. 3). It is also conceivable that the different responses for the two protrusion types to the absence of AQP0 are due to their different actin cytoskeletal configurations. As in other cell types, type 1 protrusions are likely supported by a branched actin network that is regulated by Arp2/3 protein, whereas type 2 protrusions are formed by parallel bundles of unbranched actin filaments

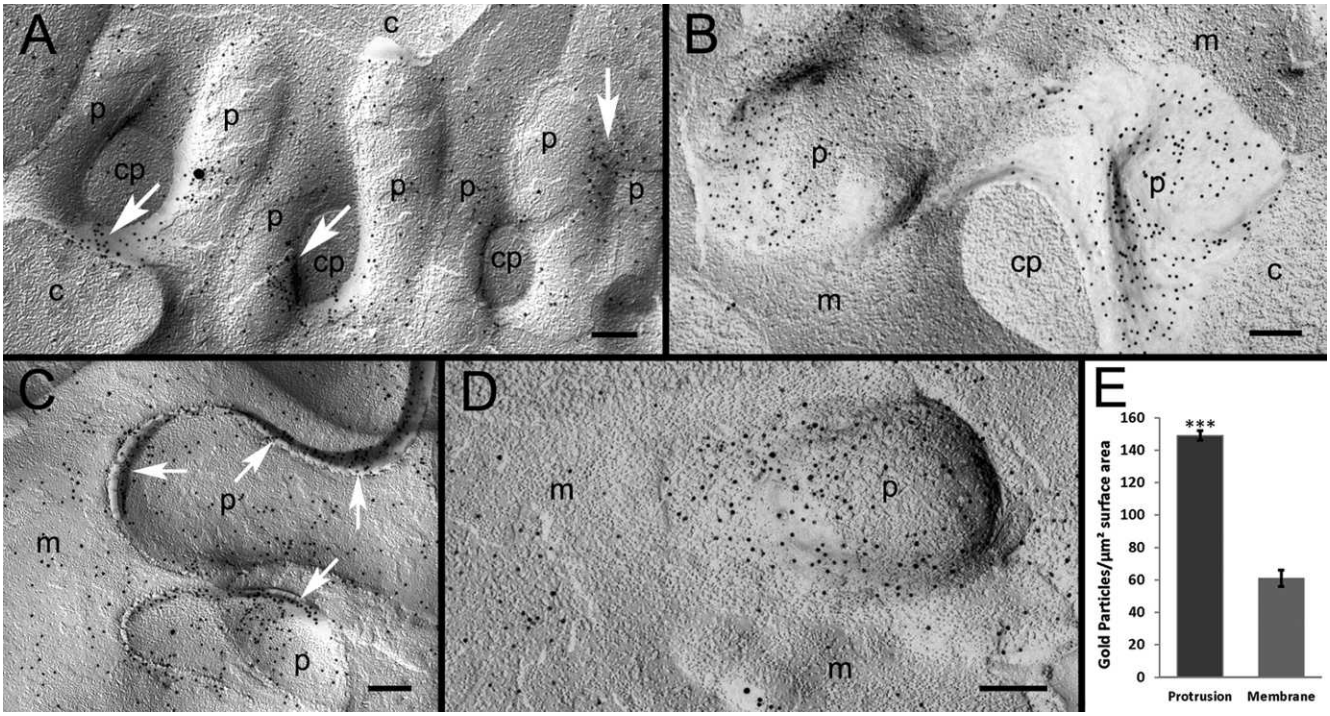

Figure 6. Preferential accumulation of AQP0 in protrusions examined with immunogold labeling. (**A**) The specific localization of AQP0 polyclonal antibody, represented by 10-nm gold particles, is observed on a cluster of protrusions (p). The rich accumulation of gold particles is distributed in the localized areas between protrusions, where they closely interlock (*arrows*). The high specificity of AQP0 labeling is evidenced in this figure, showing that the particles are localized mainly on the membrane of protrusions but not on the cytoplasm of protrusions (cp) and other cell cytoplasm backgrounds (c). (**B**) Representative labeling reveals that AQP0 is more densely labeled on protrusions (p) than the adjacent cell membranes (m). (**C**) The heavier labeling of AQP0 is also observed in the extracellular space (*arrows*) between protrusions. (**D**) In this study, quantitative analysis was conducted on micrographs (such as [**D**]) that contain both protrusions (p) and adjacent flat nonprotrusion membranes (m; see the Methods section). (**E**) A total of 5136 gold particles was counted, and the analysis showed that protrusions have significantly more gold particles than surrounding flat nonprotrusion membranes (*$P < 0.001$). *Scale bars*: 200 nm.

Investigative Ophthalmology & Visual Science

that are regulated by formins and fascin.[58–61] Under the condition without the suppression of AQP0, type 2 protrusions would be more favorable for uncontrolled elongation (Figs. 3, 4). The presence of both branched and unbranched actin filament network in the developing lens interlocking domains has been shown in an earlier study.[8]

It is notable that AQP0 has also been suggested to have an adhesion role, through its extracellular loops, to enhance gap junction coupling in superficial fibers during cell differentiation.[50] Furthermore, AQP0 is the major membrane protein of wavy square array (thin) junctions located primarily in the deep cortical fibers.[42–45] The wavy square array (thin) junctions may function to maintain the narrowed extracellular space between fiber cells to minimize light scattering. Nevertheless, the present study demonstrated that in the AQP0-deficient lens, while fiber cells are completely disrupted in the outer cortical regions, there are no intact deep cortical fibers remaining for wavy square array (thin) junctions to be formed. This further prioritizes the importance of AQP0 in targeting the interlocking protrusions for controlling the integrity and transparency of the lens during development and maturation.

Acknowledgments

The authors thank Paul FitzGerald of the University of California, Davis, California, for providing affinity-purified rabbit anti-CP49 antibody and Ross Johnson of the University of Minnesota, Minneapolis, Minnesota, for providing affinity-purified rabbit anti-bovine AQP0 polyclonal antibody. They also thank Morris Benveniste and Peter MacLeish for critical reading of the manuscript. One of the authors (W-KL) dedicates this article to his mentor and friend Clifford V. Harding Jr, who sadly passed away on May 25, 2013.

Supported by Grants EY05314 (W-KL), EY012284 (AS), and EY012085 (JXJ) from the National Eye Institute, National Institutes of Health; Welch Foundation Grant AQ-1507 (JXJ); and Grant RR03034 from the Research Centers in Minority Institutions, National Center for Research Resources, National Institutes of Health (Morehouse School of Medicine).

Disclosure: **W.-K. Lo**, None; **S.K. Biswas**, None; **L. Brako**, None; **A. Shiels**, None; **S. Gu**, None; **J.X. Jiang**, None

References

1. Kuwabara T. The maturation of the lens cell: a morphologic study. *Exp Eye Res*. 1975;20:427–443.
2. Kuszak J, Alcala J, Maisel H. The surface morphology of embryonic and adult chick lens-fiber cells. *Am J Anat*. 1980; 159:395–410.
3. Willekens B, Vrensen G. The three-dimensional organization of lens fibers in the rhesus monkey. *Graefes Arch Clin Exp Ophthalmol*. 1982;219:112–120.
4. Lo WK, Reese TS. Multiple structural types of gap junctions in mouse lens. *J Cell Sci*. 1993;106(pt 1):227–235.
5. Biswas SK, Lee JE, Brako L, Jiang JX, Lo WK. Gap junctions are selectively associated with interlocking ball-and-sockets but not protrusions in the lens. *Mol Vis*. 2010;16:2328–2341.
6. Willekens B, Vrensen G. Lens fiber organization in four avian species: a scanning electron microscopic study. *Tissue Cell*. 1985;17:359–377.
7. Kuszak JR, Macsai MS, Rae JL. Stereo scanning electron microscopy of the crystalline lens. *Scan Electron Microsc*. 1983;(pt 3):1415–1426.
8. Zhou CJ, Lo WK. Association of clathrin, AP-2 adaptor and actin cytoskeleton with developing interlocking membrane domains of lens fibre cells. *Exp Eye Res*. 2003;77:423–432.
9. Dickson DH, Crock GW. Interlocking patterns on primate lens fibers. *Invest Ophthalmol*. 1972;11:809–815.
10. Kistler J, Gilbert K, Brooks HV, Jolly RD, Hopcroft DH, Bullivant S. Membrane interlocking domains in the lens. *Invest Ophthalmol Vis Sci*. 1986;27:1527–1534.
11. Alcala J, Lieska N, Maisel H. Protein composition of bovine lens cortical fiber cell membranes. *Exp Eye Res*. 1975;21:581–595.
12. Broekhuyse RM, Kuhlmann ED, Stols AL. Lens membranes, II: isolation and characterization of the main intrinsic polypeptide (MIP) of bovine lens fiber membranes. *Exp Eye Res*. 1976; 23:365–371.
13. Takemoto LJ, Hansen JS, Nicholson BJ, Hunkapiller M, Revel JP, Horwitz J. Major intrinsic polypeptide of lens membrane: biochemical and immunological characterization of the major cyanogen bromide fragment. *Biochim Biophys Acta*. 1983; 731:267–274.
14. Johnson KR, Lampe PD, Hur KC, Louis CF, Johnson RG. A lens intercellular junction protein, MP26, is a phosphoprotein. *J Cell Biol*. 1986;102:1334–1343.
15. Horwitz J, Bok D. Conformational properties of the main intrinsic polypeptide (MIP26) isolated from lens plasma membranes. *Biochemistry*. 1987;26:8092–8098.
16. Ehring GR, Zampighi G, Horwitz J, Bok D, Hall JE. Properties of channels reconstituted from the major intrinsic protein of lens fiber membranes. *J Gen Physiol*. 1990;96:631–664.
17. Pisano MM, Chepelinsky AB. Genomic cloning, complete nucleotide sequence, and structure of the human gene encoding the major intrinsic protein (MIP) of the lens. *Genomics*. 1991;11:981–990.
18. Goodenough DA. Lens gap junctions: a structural hypothesis for nonregulated low-resistance intercellular pathways. *Invest Ophthalmol Vis Sci*. 1979;18:1104–1122.
19. Peracchia C, Girsch SJ, Bernardini G, Peracchia LL. Lens junctions are communicating junctions. *Curr Eye Res*. 1985;4: 1155–1169.
20. Johnson KR, Sas DF, Johnson RG. MP26, a protein of intercellular junctions in the bovine lens: electrophoretic and chromatographic characterization. *Exp Eye Res*. 1991;52: 629–639.
21. Mulders SM, Preston GM, Deen PM, Guggino WB, van Os CH, Agre P. Water channel properties of major intrinsic protein of lens. *J Biol Chem*. 1995;270:9010–9016.
22. Shiels A, Bassnett S. Mutations in the founder of the *MIP* gene family underlie cataract development in the mouse. *Nat Genet*. 1996;12:212–215.
23. Francis P, Chung JJ, Yasui M, et al. Functional impairment of lens aquaporin in two families with dominantly inherited cataracts. *Hum Mol Genet*. 2000;9:2329–2334.
24. Berry V, Francis P, Kaushal S, Moore A, Bhattacharya S. Missense mutations in MIP underlie autosomal dominant "polymorphic" and lamellar cataracts linked to 12q. *Nat Genet*. 2000;25:15–17.
25. Geyer DD, Spence MA, Johannes M, et al. Novel single-base deletional mutation in major intrinsic protein (MIP) in autosomal dominant cataract. *Am J Ophthalmol*. 2006;141: 761–763.
26. Wang W, Jiang J, Zhu Y, et al. A novel mutation in the major intrinsic protein (MIP) associated with autosomal dominant congenital cataracts in a Chinese family. *Mol Vis*. 2010;16:534–539.
27. Yang G, Zhang G, Wu Q, Zhao J. A novel mutation in the MIP gene is associated with autosomal dominant congenital nuclear cataract in a Chinese family. *Mol Vis*. 2011;17:1320–1323.
28. Wang KJ, Li SS, Yun B, Ma WX, Jiang TG, Zhu SQ. A novel mutation in *MIP* associated with congenital nuclear cataract in a Chinese family. *Mol Vis*. 2011;17:70–77.

29. Chandy G, Zampighi GA, Kreman M, Hall JE. Comparison of the water transporting properties of MIP and AQP1. *J Membr Biol*. 1997;159:29–39.
30. Varadaraj K, Kushmerick C, Baldo GJ, Bassnett S, Shiels A, Mathias RT. The role of MIP in lens fiber cell membrane transport. *J Membr Biol*. 1999;170:191–203.
31. Agre P, Kozono D. Aquaporin water channels: molecular mechanisms for human diseases. *FEBS Lett*. 2003;555:72–78.
32. Varadaraj K, Kumari S, Shiels A, Mathias RT. Regulation of aquaporin water permeability in the lens. *Invest Ophthalmol Vis Sci*. 2005;46:1393–1402.
33. Gonen T, Walz T. The structure of aquaporins. *Q Rev Biophys*. 2006;39:361–396.
34. Nemeth-Cahalan KL, Hall JE. pH and calcium regulate the water permeability of aquaporin 0. *J Biol Chem*. 2000;275:6777–6782.
35. Froger A, Clemens D, Kalman K, Nemeth-Cahalan KL, Schilling TF, Hall JE. Two distinct aquaporin 0s required for development and transparency of the zebrafish lens. *Invest Ophthalmol Vis Sci*. 2010;51:6582–6592.
36. Clemens DM, Nemeth-Cahalan KL, Trinh L, Zhang T, Schilling TF, Hall JE. In vivo analysis of aquaporin 0 function in zebrafish: permeability regulation is required for lens transparency. *Invest Ophthalmol Vis Sci*. 2013;54:5136–5143.
37. Gonen T, Cheng Y, Kistler J, Walz T. Aquaporin-0 membrane junctions form upon proteolytic cleavage. *J Mol Biol*. 2004;342:1337–1345.
38. Gonen T, Sliz P, Kistler J, Cheng Y, Walz T. Aquaporin-0 membrane junctions reveal the structure of a closed water pore. *Nature*. 2004;429:193–197.
39. Buzhynskyy N, Hite RK, Walz T, Scheuring S. The supramolecular architecture of junctional microdomains in native lens membranes. *EMBO Rep*. 2007;8:51–55.
40. Scheuring S, Buzhynskyy N, Jaroslawski S, Goncalves RP, Hite RK, Walz T. Structural models of the supramolecular organization of AQP0 and connexons in junctional microdomains. *J Struct Biol*. 2007;160:385–394.
41. Engel A, Fujiyoshi Y, Gonen T, Walz T. Junction-forming aquaporins. *Curr Opin Struct Biol*. 2008;18:229–235.
42. Lo WK, Harding CV. Square arrays and their role in ridge formation in human lens fibers. *J Ultrastruct Res*. 1984;86:228–245.
43. Costello MJ, McIntosh TJ, Robertson JD. Membrane specializations in mammalian lens fiber cells: distribution of square arrays. *Curr Eye Res*. 1985;4:1183–1201.
44. Costello MJ, McIntosh TJ, Robertson JD. Distribution of gap junctions and square array junctions in the mammalian lens. *Invest Ophthalmol Vis Sci*. 1989;30:975–989.
45. Zampighi GA, Hall JE, Ehring GR, Simon SA. The structural organization and protein composition of lens fiber junctions. *J Cell Biol*. 1989;108:2255–2275.
46. Zampighi GA, Eskandari S, Hall JE, Zampighi L, Kreman M. Micro-domains of AQP0 in lens equatorial fibers. *Exp Eye Res*. 2002;75:505–519.
47. Kumari SS, Varadaraj K. Intact AQP0 performs cell-to-cell adhesion. *Biochem Biophys Res Commun*. 2009;390:1034–1039.
48. Varadaraj K, Kumari SS, Mathias RT. Transgenic expression of AQP1 in the fiber cells of AQP0 knockout mouse: effects on lens transparency. *Exp Eye Res*. 2010;91:393–404.
49. Grey AC, Li L, Jacobs MD, Schey KL, Donaldson PJ. Differentiation-dependent modification and subcellular distribution of aquaporin-0 suggests multiple functional roles in the rat lens. *Differentiation*. 2009;77:70–83.
50. Liu J, Xu J, Gu S, Nicholson BJ, Jiang JX. Aquaporin 0 enhances gap junction coupling via its cell adhesion function and interaction with connexin 50. *J Cell Sci*. 2011;124:198–206.
51. Shiels A, Bassnett S, Varadaraj K, et al. Optical dysfunction of the crystalline lens in aquaporin-0–deficient mice. *Physiol Genomics*. 2001;7:179–186.
52. Jiang JX, Goodenough DA. Heteromeric connexons in lens gap junction channels. *Proc Natl Acad Sci U S A*. 1996;93:1287–1291.
53. Ireland M, Maisel H. A cytoskeletal protein unique to lens fiber cell differentiation. *Exp Eye Res*. 1984;38:637–645.
54. Alizadeh A, Clark J, Seeberger T, Hess J, Blankenship T, FitzGerald PG. Characterization of a mutation in the lens-specific CP49 in the 129 strain of mouse. *Invest Ophthalmol Vis Sci*. 2004;45:884–891.
55. Simirskii VN, Lee RS, Wawrousek EF, Duncan MK. Inbred FVB/N mice are mutant at the *cp49/Bfsp2* locus and lack beaded filament proteins in the lens. *Invest Ophthalmol Vis Sci*. 2006;47:4931–4934.
56. Broekhuyse RM, Kuhlmann ED. Lens membranes, XI: some properties of human lens main intrinsic protein (MIP) and its enzymatic conversion into a 22 000 dalton polypeptide. *Exp Eye Res*. 1980;30:305–310.
57. Gruijters WT. A non-connexon protein (MIP) is involved in eye lens gap-junction formation. *J Cell Sci*. 1989;93(pt 3):509–513.
58. Mullins RD, Heuser JA, Pollard TD. The interaction of Arp2/3 complex with actin: nucleation, high affinity pointed end capping, and formation of branching networks of filaments. *Proc Natl Acad Sci U S A*. 1998;95:6181–6186.
59. Svitkina TM, Borisy GG. Arp2/3 complex and actin depolymerizing factor/cofilin in dendritic organization and treadmilling of actin filament array in lamellipodia. *J Cell Biol*. 1999;145:1009–1026.
60. Mellor H. The role of formins in filopodia formation. *Biochim Biophys Acta*. 2010;1803:191–200.
61. Firat-Karalar EN, Welch MD. New mechanisms and functions of actin nucleation. *Curr Opin Cell Biol*. 2011;23:4–13.
62. Bagchi M, Katar M, Lo WK, Yost R, Hill C, Maisel H. ERM proteins of the lens. *J Cell Biochem*. 2004;92:626–630.
63. Rao PV, Ho T, Skiba NP, Maddala R. Characterization of lens fiber cell Triton insoluble fraction reveals ERM (ezrin, radixin, moesin) proteins as major cytoskeletal-associated proteins. *Biochem Biophys Res Commun*. 2008;368:508–514.
64. Wang Z, Schey KL. Aquaporin-0 interacts with the FERM domain of ezrin/radixin/moesin proteins in the ocular lens. *Invest Ophthalmol Vis Sci*. 2011;52:5079–5087.
65. Lo WK, Wen XJ, Zhou CJ. Microtubule configuration and membranous vesicle transport in elongating fiber cells of the rat lens. *Exp Eye Res*. 2003;77:615–626.

Investigative Ophthalmology & Visual Science